Novel Configuration for a *C*-Band Axial Vircator With High Output Power

Giacomo Migliore, Antonino Muratore, Alessandro Busacca, Pasquale Cusumano, and Salvatore Stivala

***Abstract*— We present a novel configuration for an axial virtual cathode oscillator (Vircator) operating in the *C*-band and designed for high output power applications. In order to enhance the efficiency, we have employed a geometry with up to seven reflectors along the drift space. While in previous research works this optimization process has been performed only varying the reflectors radii while using a fixed distance between reflectors, in our work we propose an optimization in terms of both reflectors radii and distances. Our optimized structure for the axial Vircator is able to provide an efficiency up to 15.6% and an output power of 1.6 GW in the *C*-band, with a working voltage of 510 kV and a cathodic current of 24 kA.**

***Index Terms*— *C*-band, high-power microwave systems, virtual cathode oscillator (Vircator).**

I. Introduction

In THE last decades, high-power microwave (HPM) systems capable of providing an output power of the order of gigawatts in the frequency range 1–10 GHz have been deeply investigated and discussed [1]. In this scenario, a device that has been extensively studied, both for the output power levels and its constructive simplicity, is the virtual cathode oscillator (Vircator) [2]–[8].

In this article, an optimized axial Vircator structure, without external magnetic field, will be discussed. Optimization will be performed by varying the reflector distances and radii, so to obtain a stable microwave signal, both in amplitude and in frequency. In what follows, preliminary theoretical considerations for addressing the study and numerical simulations carried out with the aid of Particle-in-cell (PIC)-code CST will be presented, PIC together with some considerations about the limits of the analytical evaluations.

II. Principle of Operation

A typical Vircator in the axial configuration is shown in Fig. 1 [2]. It is composed by a cathode (capable of emitting electrons), an anode (consisting of a grid permeable to electrons), a tunnel (where the interaction between the electron beam and radio frequency fields takes place), and an exit window for the radio frequency signal.

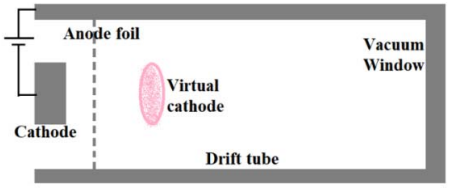

Fig. 1. Vircator in the axial configuration.

The emission of an electron beam from the cathode occurs in an explosive way due to an external voltage (few hundreds of kilovolts) applied between the cathode and the anode. The emission of the explosive type is obtained when the surface of the cathode shows some protuberances that allow to obtain an "enhancement" factor of some units of the electric field necessary for the emission due to the field effect.

Once the geometric parameters of the structure have been chosen, for a given voltage applied between cathode and anode, the space charge limited current (I_{scl}) can be calculated by means of the following relation [2]:

$$I_{\mathrm{scl}}(kA) = \frac{8.54}{1 + 2\ln\frac{R}{r_b}}\left(\gamma_0^{\frac{2}{3}} - 1\right)^{\frac{3}{2}} \tag{1}$$

where R is the radius of the output guide, r_b is the beam radius, and γ_0 is the relativistic constant at the anode, which can be calculated as

$$\gamma_0 = 1 + \frac{eV_0}{m_0 c^2} \tag{2}$$

where V_0 is the accelerating voltage, e is the electron charge, m_0 is the rest mass of the electron, and c is the speed of light.

Exceeding the limit value of the current calculated with (1) produces a downstream of the anode and, at a distance approximately equal to that between anode and cathode, a densification of electrons (virtual cathode) that oscillates both in position and in time. In addition, the electrons that are trapped between the cathode and the virtual cathode oscillate forth and back interacting with the radio frequency field.

Manuscript received 21 April 2022; accepted 13 June 2022. Date of publication 29 June 2022; date of current version 25 July 2022. The review of this article was arranged by Editor M. Blank. *(Corresponding author: Salvatore Stivala.)*

The authors are with the Department of Engineering, University of Palermo, 90128 Palermo, Italy (e-mail: salvatore.stivala@unipa.it).

Color versions of one or more figures in this article are available at https://doi.org/10.1109/TED.2022.3184917.

Digital Object Identifier 10.1109/TED.2022.3184917

In what follows, the mechanism that presides over the formation of the virtual cathode and its oscillation in space and time will be discussed in more detail.

The electrons emitted by the cathode and accelerated toward the anode go beyond it (because of its transparency to the electrons) and move in the area bounded by the anode and the tube. If the emitted current exceeds the space charge limited current, an intense cloud of electrons is formed at a distance from the anode roughly equal to the distance between the anode and the cathode. This cloud (virtual cathode) reaches its maximum density, and further electrons coming from the cathode are reflected back (reflex electrons). Obviously, the repulsion forces inside the virtual cathode tend to reduce the density of the electrons (oscillation over time), and therefore, the negative potential of the virtual cathode tends to reduce, making the virtual cathode move toward the anode (oscillation in space). At that point, the electrons coming from the cathode encountering a smaller repulsion force refeed the virtual cathode, which tends to move away from the anode to repeat the cycle.

The presence of a variable electric field inside the cavity interacts with this movement of charges resulting in a variation in density and therefore in a dynamic current that increases the variable electric field (main effect).

The reflected electrons, due to the considerable repulsion forces provided by the virtual cathode, undergo a speed modulation, due to the oscillatory movement of the virtual cathode, which results in a modulation of density and therefore in a dynamic current that interacts with the electric field variable in the area between the virtual cathode and the anode giving rise to an increase in the electric field at a frequency generally different from that of the field generated by the virtual cathode (reflex frequency).

As already discussed, the necessary condition for the formation of a virtual cathode is the exceeding of the space charge limited current calculated with (1). The virtual cathode oscillations occur at a frequency close to the plasma oscillation frequency (f_{osc}) that can be approximated by the following formula [5]:

$$f_{\text{osc}} = \frac{4.77}{d} \ln\left(\gamma_0 + \sqrt{\gamma_0^2 - 1}\right) \tag{3}$$

where d is the anode–cathode distance.

The electrons that are unable to reach the virtual cathode (reflex electrons) oscillate around the anode back and forward at a frequency that can be calculated by means of the following formula [1]:

$$f_{\text{ref}} = \frac{\sqrt{V_0}}{4d}\sqrt{\frac{ec^2}{2m_0c^2 + eV_0}}. \tag{4}$$

In general, the frequency of the reflex oscillations is lower than the frequency of the virtual cathode oscillations.

III. Efficiency

In the previous paragraph, we have reported the relations that allow to calculate, albeit with the due approximations and hypotheses, some fundamental parameters related to the Vircator.

To the best of our knowledge, the studies conducted so far do not report theoretical results about the efficiency and, therefore, the output power.

An important approach has been reported in an article by Jiang [10], where the presence of an external electric field $E'(t) = E'_0\sin(\omega t)$ is assumed and added to the field due to the presence of the virtual cathode $E(t)$. The efficiency values (defined as the ratio between the generated RF power and the dc input power) reported in this article can be expressed as a function of the ratio $A = E'_0/E$.

It is known that in an oscillator, a noise signal, always present, is gradually amplified until it reaches a maximum value, which defines the stable equilibrium state of the oscillator. The parameters limiting the value of the output signal are intrinsic to the oscillator and are due to the nonlinearities occurring in the mechanism that presides over the amplification.

The efficiency values obtained do not allow to calculate the output power, since the latter is a function of E'_0 (that we do not know). To properly calculate the output power and efficiency, it is necessary a numerical analysis using software like CST or MAGIC. All simulations shown in this article have been performed by means of CST microwave studio.

IV. Oscillator Design

The proposed Vircator has been designed employing a circular waveguide structure, whose radius and length have been chosen starting from the desired oscillation frequency (f_{osc}) set equal to 3.5 GHz. As regard the radius, following the results reported in [11] and [12], we have chosen a value able to guarantee the maximum generated power supported by the TM_{01} mode at the operating frequency. Following this consideration, the radius of the waveguide (r_w) has been chosen equal to 6.6 cm.

As regard the length of the waveguide, it has been set equal to about five times the guide wavelength (λ_g), the latter being calculated as follows:

$$\lambda_g = \frac{c}{f_{\text{osc}}\sqrt{1 - \left(\frac{f_c}{f_{\text{osc}}}\right)^2}} \tag{5}$$

where f_c is the cutoff frequency of the TM_{01} mode.

The anode–cathode distance has been obtained from (3).

In order to increase the output power of the Vircator, a multistage architecture has been employed, introducing several reflectors, whose distances (d_{ref}) and radius (r_{ref}) have been obtained starting from the formula for a TM_{011} mode in a cylindrical cavity

$$f_{\text{osc}} = f_{\text{TM}_{011}} = \frac{c}{2\pi}\sqrt{\left(\frac{2.405}{r_{\text{ref}}}\right)^2 + \left(\frac{\pi}{d_{\text{ref}}}\right)^2}. \tag{6}$$

The region comprised between two consecutive reflectors, in fact, acts like a pseudocavity [13]. Moreover, since each virtual cathode acts like an emitter for the following reflector, the distance between two consecutive reflectors has to be equal at least two times the anode–cathode distance. Once chosen the radius of the waveguide, an optimization in terms of the

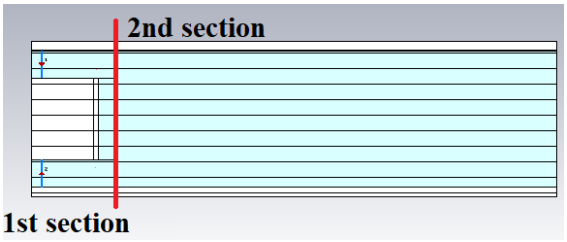

Fig. 2. Proposed structure of the axial Vircator for CST simulations.

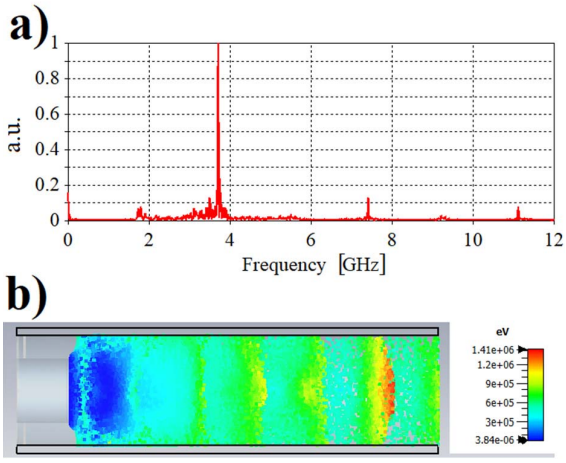

Fig. 3. (a) Spectrum of the output signal in arbitrary unit. (b) Particles energy and virtual cathode formation.

reflectors radii and distances has been performed, as described in the following section.

The input coaxial cable connected to the cathode has been chosen with an external cable radius equal to the radius of the output waveguide, while the inner cable radius has been set equal to the cathode radius, which was empirically optimized by the simulation software.

V. PIC Simulations

We first simulated a single anode axial Vircator structure. It consists of a first section that is basically a 6-cm-long coaxial cable with an external radius of 6.6 cm and an inner radius of 3.9 cm, value corresponding to the optimized cathode radius. This first section is connected to a second one, which is a circular waveguide with the same external radius and a length of about 45 cm, with a single anode at a distance of 1.6 cm from the cathode (as shown in Fig. 2).

The cathode is characterized by an explosive emission and is placed at the edge of the coaxial structure, while the anode has been set with a sheet transparency of 100%. The cathode is supplied by four discrete ports placed at the beginning of the coaxial waveguide, employing a pulsed voltage of 511 kV, with a pulse duration of 50 ns and a rising time of 5 ns (to allow the formation of the virtual cathode). Numerical simulation for the single anode axial Vircator structure provided a mean RF power output of about 50 MW at a frequency of 3.72 GHz, with a current of about 23.5 kA, reaching an efficiency of 0.42%. The shift of the numerically simulated frequency, with

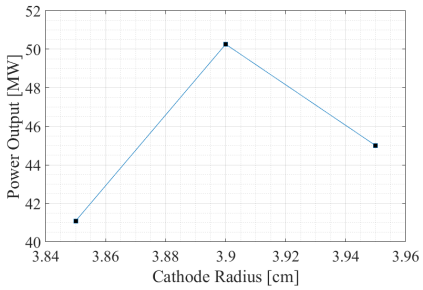

Fig. 4. Power output as a function of the cathode radius.

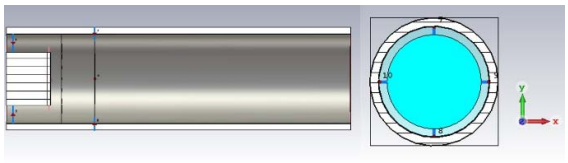

Fig. 5. Lateral (left) and frontal (right) sections of the considered structure.

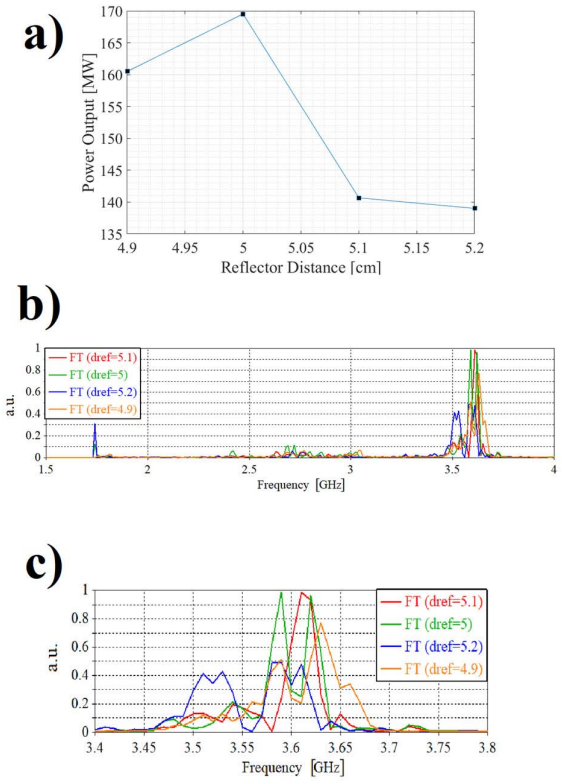

Fig. 6. (a) Output power as a function of the reflector distance. (b) Fourier transform of the output signal with respect to the reflector distance. (c) Zoomed-in view of the Fourier transform.

respect to the theoretical value [calculated with (3), and equal to 3.92 GHz], is due to the approximation of the applied formula, in which the dependence from the circular waveguide diameter is not taken into account. Fig. 3(a) shows the spectrum of the output signal with a narrow peak at 3.72 GHz and two lower peaks at multiple frequencies. Fig. 3(b) shows

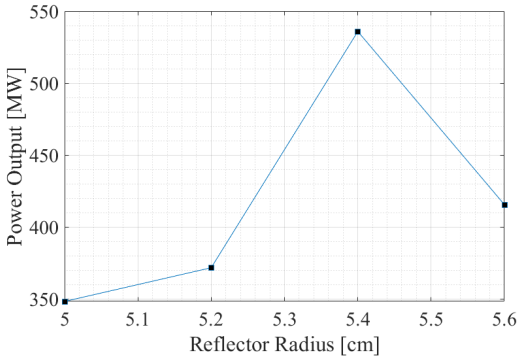

Fig. 7. Power output as a function of the second reflector radius.

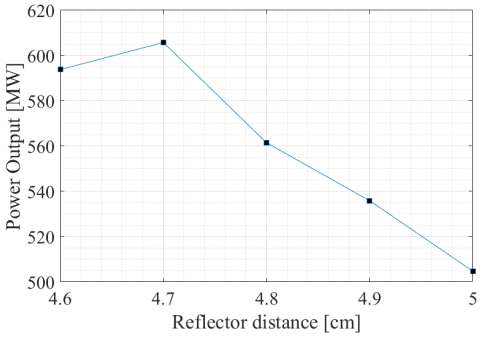

Fig. 8. Power output as a function of the reflector distance.

TABLE I
REFLECTOR RADIUS AND ITS DISTANCE WITH RESPECT TO THE PREVIOUS ONE

	Radius	Distance
1° Reflector	5.6 cm	5 cm
2° Reflector	5.4 cm	4.7 cm
3° Reflector	4.5 cm	4.7 cm
4° Reflector	3.5 cm	4.7 cm
5° Reflector	2.7 cm	4.5 cm

the particles energy and the formation of the virtual cathode, at approximately two times the anode–cathode distance.

As already discussed, an optimization in terms of cathode radius has been performed, by varying it up to ±0.5 mm. The better values of power output and efficiency are reached with a radius of 3.90 cm. As shown in Fig. 4, the power output results to be very sensitive with this variation: a power drop has been obtained, in fact, in both directions.

VI. OPTIMIZATION PROCESS

According to [11] and [12], in order to enhance the efficiency of the Vircator, several reflectors can be introduced, thus allowing the formation of multiple virtual cathodes. Such reflectors are transparent to electrons, while they interact with electromagnetic fields and allow a mutual electromagnetic coupling due to their peripheral slots. The multiple virtual cathodes, if optimized in terms of reflectors radii and distances, oscillate at the same frequency of the original one. While in the abovementioned articles [11], [12], this optimization

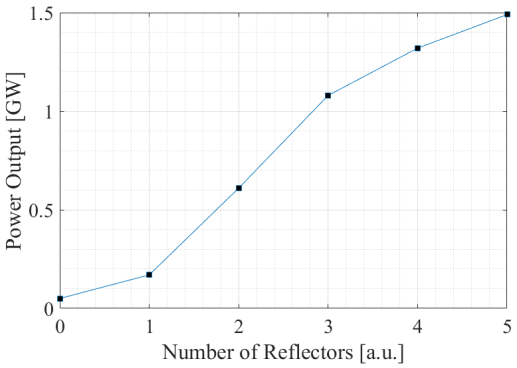

Fig. 9. Power output as a function of number of reflectors.

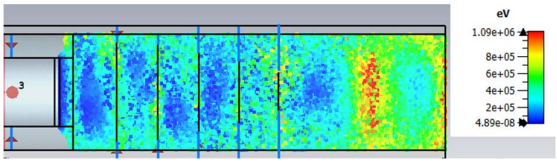

Fig. 10. Particle energy with five reflectors at 50 ns (last frame of the simulation).

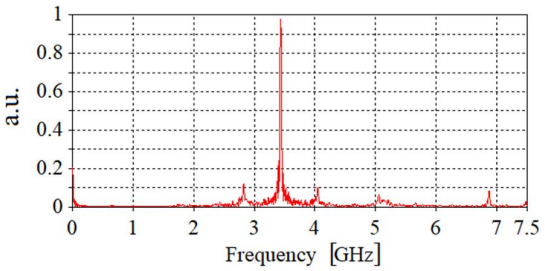

Fig. 11. Fourier transform of the output signal with five reflectors.

process has been performed only varying the reflectors radii while using a fixed reflectors distance, in our work, we propose an optimization in terms of both reflectors radii and distances. Moreover, we demonstrate that it is possible to introduce more than five reflectors without increasing the TE_{11} mode, simply adjusting the reflectors radii.

The distance between two consecutive reflectors has been tuned step by step, introducing only one reflector at a time. The first reflector was introduced at a distance of 5 cm from the anode and with radius over the 75% of the anode radius connected to the circular guide by four discrete ports, so to have the same potential difference (as shown in Fig. 5).

At first, radius variations of 1 mm in the range 5.2–5.7 cm have been studied: a maximum mean output power of 169 MW has been reached with a radius value of 5.6 cm.

Subsequently, the distance of the reflector with respect to the anode was varied with steps of 1 mm in the range 4.9–5.2 cm. Our simulations have shown that the best results in terms of output power can be obtained at a distance of 5 cm. In Fig. 6, the output power and the frequency spectrum as a function of the reflector distance are shown: the correlation between the optimization in terms of distance and the frequency peak is evident, also the dependence of the RF propagation mode.

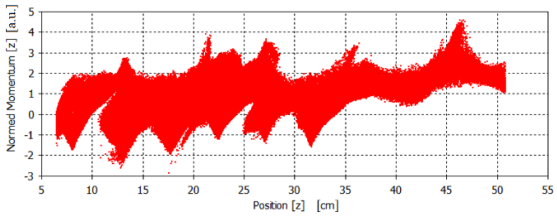

Fig. 12. Particles momentum.

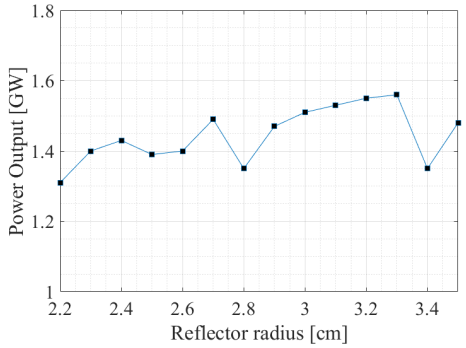

Fig. 13. Power output versus sixth reflector radius.

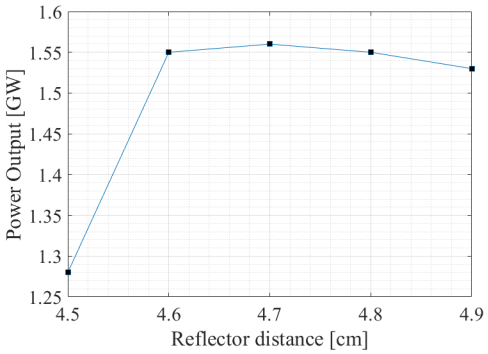

Fig. 14. Output power as a function of the sixth reflector distance.

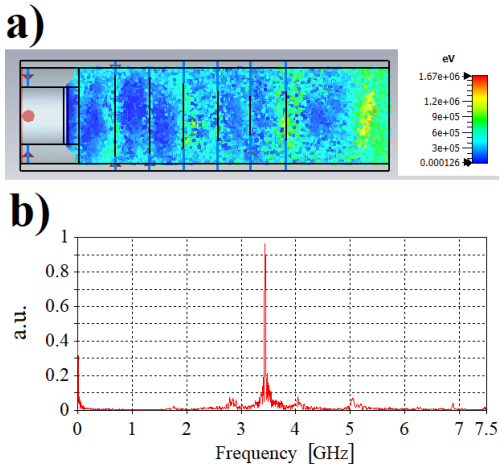

Fig. 15. (a) Particle preview with reflectors profile and virtual cathodes formation. (b) Spectrum of the output signal in arbitrary unit.

The efficiency obtained in this condition is of 1.43% with a current of about 24 kA.

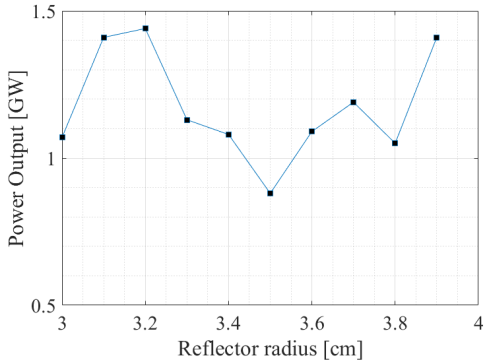

Fig. 16. Output power as a function of the seventh reflector radius.

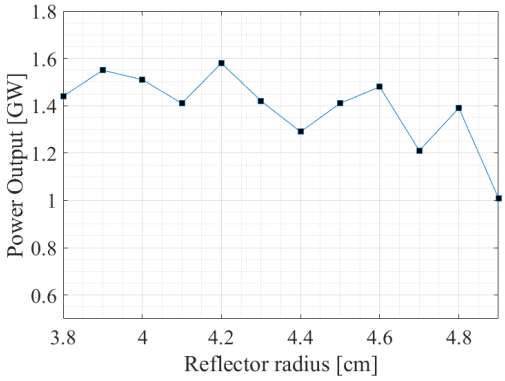

Fig. 17. Power output versus seventh reflector radius.

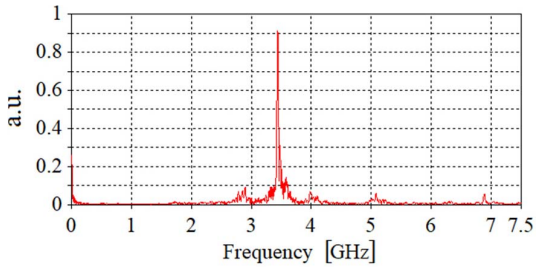

Fig. 18. Fourier transform of the output signal in arbitrary unit with seven reflectors.

Subsequently, we performed a new set of simulations, with the addition of a second reflector, 4.9 cm distant from the first one and whose radius was varied in the range 5–5.6 cm with steps of 2 mm. In these conditions, as shown in Fig. 7, the optimum in terms of mean power output (535 MW) was obtained with a radius of 5.4 cm.

The optimum in terms of reflector distance this time was reached reducing the distance to 4.7 cm, as shown in Fig. 8, reaching a mean power output of 605.8 MW with an efficiency of 5.4%.

In a similar way, we have gradually added three more reflectors. The new structure, with a total number of five reflectors, was optimized in terms of reflectors radii and distances, which are reported in Table I.

The mean power output as a function of the number of reflectors is shown in Fig. 9. The structure with five reflectors

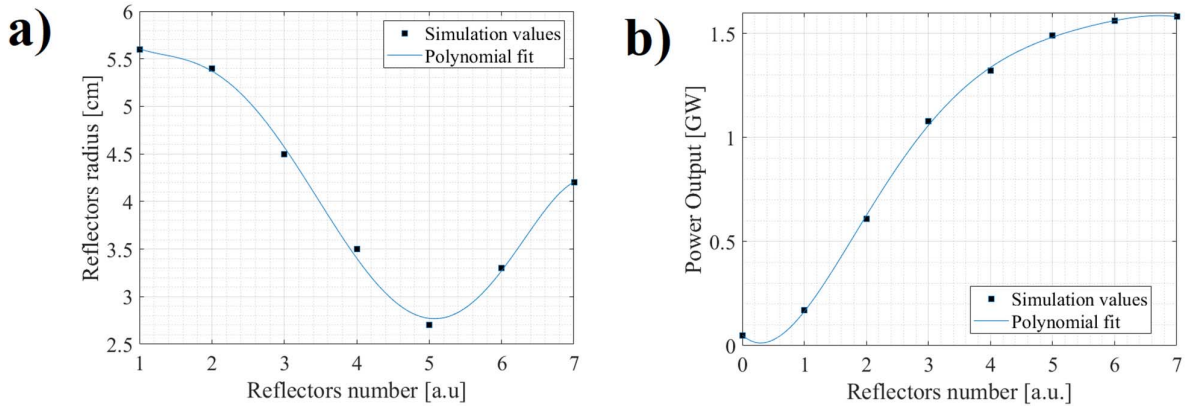

Fig. 19. (a) Reflector radius versus reflectors number: simulated values (dots) and fitting curve with a polynomial approximation of the fifth order (solid line). (b) Power output versus reflectors number.

is able to reach a mean power output of 1.5 GW with an efficiency of about 14.52%.

Fig. 10 displays the simulated particles energy within the structure. The formation of six virtual cathodes, each at almost two times the anode–cathode distance, can be observed.

The RF spectrum (see Fig. 11) shows a narrow maximum peak at 3.43 GHz and two lesser peaks at the double and triple frequencies.

The particles momentum distribution (see Fig. 12) confirms the presence of the six virtual cathodes, each of them characterized by zero momentum after any reflector.

VII. Novel Configuration

As already anticipated, in this work, we propose a novel structure, optimized in terms of both reflectors radii and distances and employing more than five reflectors.

The sixth reflector was placed at a distance of 4.7 cm with respect to the fifth one. An optimization in terms of reflector radius was performed by varying it from 2.2 up to 3.5 cm with a step of 1 mm. Fig. 13 shows the result of this sweep simulation, demonstrating that the optimum value is 3.3 cm.

Once the radius value has been chosen, the reflector distance has been varied from 4.5 to 4.9 cm with a step of 1 mm. The structure performance is optimized with a reflector at a distance of 4.7 cm (as shown in Fig. 14), thus providing a power output of 1.56 GW, an efficiency of 15.3%, and a current of 23.94 kA.

The profile of the structure with six reflectors is represented in Fig. 15(a), where the virtual cathodes formation is also evident. Fig. 15(b) shows the frequency spectrum of the output signal, still narrow and centered at the frequency of 3.45 GHz.

In order to further increase the output power and efficiency, two more reflectors have been added, adjusting their radii to avoid the increase of the TE_{11} mode. In fact, unlike what already reported in [11] and [12], it has been found that by increasing the radius of both reflectors, it is still possible to increase the output power of the Vircator, reaching a sort of saturation with the seventh reflector, while preserving the power output almost completely on the TM_{01} mode.

At first, the seventh reflector was placed at a distance of 4.6 cm from the sixth one (reaching a total distance from the anode of 33 cm), almost at the end of the waveguide. In such a position, the presence of the reflector interferes with the RF signal. In fact, as shown in Fig. 16, by varying the radius of the reflector from 3 up to 3.9 cm, the output power results to be always lesser than the case with six reflectors.

TABLE II
Reflectors Radii and Distances

	Radius	Distance
6° Reflector	3.3 cm	4.7 cm
7° Reflector	4.2 cm	4.8 cm

Even changing the distance of the reflector, the result did not change. For this reason, the length of the circular waveguide has been increased of about one-time λ_g. In this condition, the reflector radius was varied from 3.8 up to 4.9 cm, fixing the distance to 4.8 cm.

As shown in Fig. 17, the maximum power has been obtained with a radius of 4.2 cm, reaching a power output of 1.58 GW and an efficiency of 15.6% that is the highest obtained value that we obtained at this frequency.

As shown in Fig. 18, the frequency spectrum is still a very narrow and centered at 3.45 GHz, with few lower peaks that are higher than the configuration with only six reflectors.

In Table II, the optimal radii and distances of sixth and seventh reflectors are reported.

In conclusion, Fig. 19 shows the profile of each reflector as a function of the distance and the corresponding power output. A strong saturation effect can be observed, thus demonstrating that adding more than seven reflectors would be almost useless.

VIII. Conclusion

In this article, an optimization in terms of number of reflectors, their distances, and radii in an axial Vircator has been performed. The results show that each pair of reflectors acts like a pseudocavity for the RF signal. For this reason, a tuning in terms of radius is not enough, but also an optimization of the distance between each reflector is necessary to obtain better results in terms of efficiency and output power. With respect to previous results reported in the literature, in order to increase

the output power and efficiency, two more reflectors have been added; their dimensions have been adjusted to avoid the increase of the TE_{11} mode. In fact, we have demonstrated that by increasing the radii of both the two reflectors with a value comparable to the fourth and third reflectors, respectively, it is still possible to increase the output power of the Vircator reaching a sort of saturation with the seventh reflector. From this study, it does not seem convenient to increase the number of reflectors more than seven because there are not advantages in terms of power output and efficiency. The results obtained, i.e., power output of 1.6 GW and efficiency of 15.6%, are very interesting for the applications of this device.

REFERENCES

[1] J. J. A. B. Swegle and E. Schamiloglu, "High power microwaves applications," in *High Power Microwaves*, 3rd ed. Boca Raton, FL, USA: CRC Press, Nov. 2015, pp. 41–91, doi: 10.1201/b19681.

[2] C. Müller, "Design and experiments with high power microwave sources," Ph.D thesis, Dept. KTH Rymd-och plasmafysik Skolan för elektro-och systemteknik, KTH Electr. Eng., Stockholm, Sweden, 2012. [Online]. Available: https://www.diva-portal.org/smash/get/diva2:567419/FULLTEXT01.pdf

[3] M. Maiti, D. Tiwari, A. Roy, N. Singh, and S. Wagh, "Simulation and analysis of an axial vircator using PIC code," in *Proc. Asia–Pacific Symp. Electromagn. Compat. (APEMC)*, May 2015, pp. 172–176, doi: 10.1109/APEMC.2015.7446235.

[4] W. Jiang, K. Masugata, and K. Yatsui, "Mechanism of microwave generation by virtual cathode oscillation," *Phys. Plasmas*, vol. 2, no. 3, pp. 982–986, Mar. 1995, doi: 10.1063/1.871377.

[5] A. Wymysłowski, "Vircator—Analytical and numerical analysis and optimization of A vacuum microwave high power device," *Int. J. Res. Granthaalayah*, vol. 6, no. 5, pp. 47–53, May 2018, doi: 10.29121/granthaalayah.v6.i5.2018.1422.

[6] R. F. Hoeberling and M. V. Fazio, "Advances in virtual cathode microwave sources," *IEEE Trans. Electromagn. Compat.*, vol. 34, no. 3, pp. 252–258, Aug. Aug. 1992, doi: 10.1109/15.155837.

[7] A. E. Dubinov and V. D. Selemir, "Electronic devices with virtual cathodes (review)," *J. Commun. Techn. Electr.*, vol. 47, no. 6, pp. 575–600, 2002.

[8] V. D. Selemir, A. E. Dubinov, V. V. Voronin, and V. S. Zhdanov, "Key ideas and main milestones of research and development of microwave generators with virtual cathode in RFNC-VNIIEF," *IEEE Trans. Plasma Sci.*, vol. 48, no. 6, pp. 1860–1867, Jun. 2020, doi: 10.1109/TPS.2020.2974868.

[9] W.-Y. Woo, "Two-dimensional features of virtual cathode and microwave emission," *Phys. Fluids*, vol. 30, no. 1, pp. 239–244, Jan. 1987, doi: 10.1063/1.866181.

[10] W. Jiang and M. Kristiansen, "Theory of the virtual cathode oscillator," *Phys. Plasmas*, vol. 8, no. 8, pp. 3781–3787, Aug. 2001, doi: 10.1063/1.1382643.

[11] S. Champeaux, P. Gouard, R. Cousin, and J. Larour, "3-D PIC numerical investigations of a novel concept of multistage axial vircator for enhanced microwave generation," *IEEE Trans. Plasma Sci.*, vol. 43, no. 11, pp. 3841–3855, Nov. 2015, doi: 10.1109/TPS.2015.2477561.

[12] S. Champeaux, P. Gouard, R. Cousin, and J. Larour, "Improved design of a multistage axial vircator with reflectors for enhanced performances," *IEEE Trans. Plasma Sci.*, vol. 44, no. 1, pp. 31–37, Dec. 2015, doi: 10.1109/TPS.2015.2502432.

[13] J. Benford, D. Price, H. Sze, and D. Bromley, "Interaction of a vircator microwave generator with an enclosing resonant cavity," *J. Appl. Phys.*, vol. 61, no. 5, pp. 2098–2100, Mar. 1987, doi: 10.1063/1.337965.